

Re-investigation of heat capacity and pairing phase transition in hot $^{93-98}\text{Mo}$ nuclei

Le Thi Quynh Huong^{1,a}, Tran Dong Xuan^{2,3}, Nguyen Ngoc Anh⁴, Nguyen Quang Hung^{2,3,b}.

¹Department of Natural Science and Technology, Khanh Hoa University, Nha Trang City, Khanh Hoa Province, Vietnam

²Institute of Fundamental and Applied Sciences, Duy Tan University, Ho Chi Minh City 700000, Vietnam

³Faculty of Natural Sciences, Duy Tan University, Danang City 550000, Vietnam

⁴Dalat Nuclear Research Institute, Vietnam Atomic Energy Institute, 01 Nguyen Tu Luc, Dalat City 670000, Vietnam

Received: date / Accepted: date

Abstract The empirical heat capacities of $^{93-98}\text{Mo}$ nuclei are re-investigated by using the latest updated and recommended nuclear level density (NLD) data below the neutron binding energy B_n combined with the back-shifted Fermi-gas (BSFG) model for the energy region above B_n . For the latter, the BSFG formula with energy-dependent level density parameter is used and the new parameterization has been carried out in order to obtain the best fit to the new NLD data in the whole data range. The results obtained show that the S-shaped heat capacity, a fingerprint of the pairing phase transition, is more pronounced in even $^{94,96,98}\text{Mo}$ nuclei than that in odd $^{93,95,97}\text{Mo}$ isotopes. This result is different with those obtained in two previous studies by R. Chankova et al., [Phys. Rev. C **73**, 034311 (2006)] and K. Kaneko et al., [Phys. Rev. C **74**, 024325 (2006)], in which the old NLD data and the BSFG model with energy-independent level density parameter were used. Moreover, the present work suggests that the very strong S-shape observed in the heat capacities of both even and odd Molybdenum isotopes by K. Kaneko et al., [Phys. Rev. C **74**, 024325 (2006)] should be re-investigated. The present work also suggests that obtain the correct heat capacity and associated pairing phase transition in excited nuclei, one should use the correct NLD data and the best fitted BSFG NLD in the entire region where the experimental data are available.

Keywords Nuclear level density · Back-shifted Fermi-gas model · Empirical heat capacity · Hot $^{93-98}\text{Mo}$ nuclei

1 Introduction

The nuclear level density (NLD), which was first introduced as the number of excited levels per unit of excitation energy [1], is known to play a major role in studying not only nuclear structure and reactions, but also nuclear astrophysics [2,3]. It also reflects the average properties of excited nuclei such as thermodynamic quantities (excitation energy, free energy, entropy, heat capacity, etc.) and/or quantum phase transition [4]. In principle, the thermodynamic properties of a nucleus can be directly extracted from the experimental NLD data by using two statistical ensembles, namely the canonical ensemble (CE) and microcanonical ensemble (MCE) as atomic nucleus is a system with a fixed number of particles [5,6,7]. However, there are some ambiguities with the use of MCE since the experimental NLD is discrete and covers the excitation energy E below the neutron binding energy B_n (~ 8 MeV) only [8, 9,10,11,12]. For example, the nuclear temperature T extracted from the experimental NLD data using the MCE can even become unphysically negative [13,14]. Hence, the CE is often used to describe the nuclear thermodynamic properties instead of the MCE. Within the CE, the experimental NLD is extrapolated, by using the back-shifted Fermi-gas (BSFG) model [15], to cover the excitation energy above B_n and up to 150 MeV. The experimental plus BSFG NLD is then used to construct the CE partition function $Z_{\text{CE}}(T)$ based on which all the nuclear thermodynamic quantities are calculated [16,17].

Among the nuclear thermodynamic quantities extracted from the CE, the heat capacity, which characterizes the variation of E with T , contains the information on the phase transition from a phase with strong pairing correlations to that with weak pairing ones via

^aCorresponding author; e-mail: lethiquynhhuong@ukh.edu.vn

^bCorresponding author; e-mail: nguyenvquanghung5@duytan.edu.vn

its S-shaped curve [18, 19, 20, 21, 22, 23, 24]. However, the relation between this feature of heat capacity found in hot nuclei and the odd-even mass differences still remains disagreement. For example, the very unusually strong S-shaped heat capacities have been reported in a series of $^{93-98}\text{Mo}$ nuclei in Ref. [22], which are quite different from those reported previously in Ref. [21] using the same NLD data of the same nuclei. Moreover, the NLD data of these nuclei have been recently re-analyzed and updated in Ref. [25] based on a simultaneous analysis of the (γ, n) and (n, γ) reactions in which the NLD is one of the most important inputs. Hence, the heat capacities in these $^{93-98}\text{Mo}$ should be re-investigated to have a precise description of the pairing phase transition in these isotopes. This is the goal of the present paper.

2 Formalism

2.1 The back-shifted Fermi-gas model

The first NLD model, which was proposed long time ago by Bethe in 1937 [1], is the Fermi-gas (FG) model. This model was derived based on an assumption that the single-particle states, from which the excited levels of the nucleus are constructed, are equally spaced. This simple assumption of the FG model is not enough to describe the NLD of excited nuclei in which several structures such as pairing correlation, shell effect, deformation, collective and rotational excitations, etc., are known to have significant contribution to the NLD. Hence, an extension of the FG model, called the back-shifted Fermi gas (BSFG) model, was proposed in Ref. [15], in which most of important structures of excited nuclei are taken into account. The BSFG formula has the form as

$$\rho_{\text{BSFG}}(E) = \frac{\exp\left[2\sqrt{a(E-E_1)}\right]}{12\sqrt{2}\sigma a^{1/4}(E-E_1)^{5/4}}, \quad (1)$$

where a is the level density parameter; E is the excitation energy; E_1 is the back-shifted energy, which is considered to be a free parameter determined by fitting to the data of each nucleus. The spin cut-off parameter σ in Eq. (1) is given as

$$\sigma^2 = 0.0888A^{2/3}\sqrt{a(E-E_1)}, \quad (2)$$

with A being the mass number.

The most important parameter in the BSFG formula (1) is the level density parameter a , which determines the slope of the NLD curve. In general, a is assumed to be constant, whose values can be obtained

from the systematic fitting to the experimental average level spacing D_0 data of a number of excited nuclei [26, 27]. However, microscopic NLD calculations have shown that the level density parameter a should depend on the excitation energy [28, 29]. Moreover, the shell effect, which is large at low-excitation energy and damped at high-excitation energy, should be also taken into account [30]. The energy-dependent level density parameter a taking into account the damping of the shell effect can be described by the a phenomenological formula as follows [28]

$$a \equiv a(Z, A, E) = \tilde{a}(A) \left\{ 1 + \frac{\delta W(Z, A)}{E - E_1} [1 - e^{-\gamma(E-E_1)}] \right\}, \quad (3)$$

where $\tilde{a}(A)$ is the asymptotic level density obtained when all the shell effects are damped, whereas $\delta W\{Z, A\}$ is the shell-correction energy defined as

$$\delta W(Z, A) = M_{\text{exp}} - M_{\text{LD}}, \quad (4)$$

with M_{exp} and M_{LD} being the experimental mass and the mass calculated by using the macroscopic liquid-drop formula, respectively. The damping parameter γ in Eq. (3), which determines how rapidly $a(Z, A, E)$ approaches $\tilde{a}(A)$, is given as

$$\gamma = \frac{\gamma_0}{A^{1/3}}, \quad (5)$$

where γ_0 is the global parameter obtained from the fittings to the experimental data over a whole range of mass numbers.

There is another version of the BSFG formula, which has been used in the normalization procedure of the experimental NLD within the Oslo technique (see e.g., Refs. [20, 21, 22]). In this version, the level density parameter is assumed to be energy-independent. Therefore, to have the best fit to the experimental NLD data, an additional fitting parameter η is used, namely

$$\rho_{\text{BSFG}}(E) = \eta \frac{\exp\left[2\sqrt{a(E-E_1)}\right]}{12\sqrt{2}\sigma a^{1/4}(E-E_1)^{5/4}}, \quad (6)$$

where σ is the same as Eq. (2); $a = 0.21A^{0.87}$; and $E_1 = C_1 + E_{\text{pair}}$ with $C_1 = -6.6A^{-0.32}$ and E_{pair} being the pairing energy. The parameter η is adjusted in order to reproduce the experimental D_0 data [22]. This version of BSFG formula is only used to connect the NLD data in the intermediate energy region from ~ 4 to $(B_n - 1)$ MeV to the NLD data at $E = B_n$. Therefore, for the overall description of the NLD data in the whole energy region, the use of formula (1) (with the energy-dependent a) should be always better than that of Eq. (6) (with the energy-independent a). For instance, the

BSFG with energy-dependent a has been widely used in the normalization procedure within the Oslo method since 2013 (see e.g., Refs. [31,32]), whereas the BSFG with energy-independent a was only used before that (see e.g., Refs. [20,21]).

2.2 Thermodynamic quantities

Having a highly dense state density, even at low-excitation energy, an atomic nucleus can be well described by a statistical ensemble [5,6]. Hence, the NLD has a direct relation to the thermodynamic partition function, which characterizes the statistical properties of a system in thermodynamic equilibrium. As discussed in the Introduction, the canonical ensemble (CE) is often used to describe the nuclear thermodynamic properties.

Within this ensemble, the CE partition function $Z(T)$ can be calculated from the NLD making use of the inverse Laplace transform of the NLD, namely [33]

$$Z(T) = \sum_{E_i=0}^{\infty} \rho(E_i) e^{-E_i/T} \delta E_i, \quad (7)$$

where $\rho(E_i)$ is the total NLD at a given excitation energy E_i ; δE_i is the energy bin; and T is nuclear temperature. Based on the CE partition function (7), we can easily calculate all the thermodynamic quantities such as free energy $F = -T \ln Z$, entropy $S = -\partial F / \partial T$, total energy $\bar{E} = F + TS$, and heat capacity $C = \partial \bar{E} / \partial T$.

It is worthwhile to mention that the summation in Eq. (7) should be taken from $E_i = 0$ to $E_i \rightarrow \infty$, that is, the NLD $\rho(E_i)$ must be extended up to very high-excitation energy. However, the experimental NLD data are usually limited below the neutron binding energy B_n . Hence, the BSFG model (1) is used to extend the NLD to above B_n and up to 120 MeV. This choice of maximum E_i is enough for the study of nuclear thermodynamics within a temperature range from 0 to 2 MeV [34,35]. Consequently, the summation in Eq. (7) is split into two parts, namely

$$Z(T) = \sum_{E_i=0}^{E_i < B_n} \rho_{\text{exp}}(E_i) e^{-E_i/T} \delta E_i + \sum_{E_i=B_n}^{E_i=120 \text{ MeV}} \rho_{\text{BSFG}}(E_i) e^{-E_i/T} \delta E_i, \quad (8)$$

where the first part is related to the experimental NLD data (ρ_{exp}), while the second part is associated to the BSFG NLD (ρ_{BSFG}). The thermodynamic quantities obtained from the partition function (8) are often called the experimental or empirical ones, which are used to compare with the theoretical calculations (see e.g., Refs. [20,21,22,34,35]).

3 Numerical results and discussion

Six medium-mass $^{93-98}\text{Mo}$ nuclei, whose experimental NLD data are available in Refs. [21,25,36], have been selected in the present work. Regarding the experimental NLD data, the first datasets for two $^{96,97}\text{Mo}$ nuclei were available in 2003 using the (^3He , $^3\text{He}'$) reactions [36]. The later experiments using both (^3He , $^3\text{He}'$) and (^3He , α) reactions in 2006 provided another datasets for all $^{93-98}\text{Mo}$ nuclei [21]. In the latest experimental study in 2013, the previous NLD data of $^{94-98}\text{Mo}$ have been re-analyzed by self-consistently combining the photoabsorption cross-section data obtained within the (^3He , $^3\text{He}'$) and (^3He , α) reactions with those taken from the (n , γ) and (γ , n) experiments [25]. In the latest experiment, an adopted range for the D_0 values of $^{94-98}\text{Mo}$, based on which the experimental NLD data were normalized, has been proposed. This range includes the minimum D_0^{min} , maximum D_0^{max} , and recommended D_0^{rec} values [25] and the new NLD datasets normalized using those D_0 values are provided and accessible via Ref. [37]. In the present work, the recommended D_0^{rec} and its associated NLD data have been used.

Table 1 Parameters of the BSFG formula (6) used in Refs. [21,22]

Nucleus	E_{pair} (MeV)	a (MeV $^{-1}$)	C_1 (MeV)	η	D_0 (eV)
^{93}Mo	0.899	10.83	-1.547	0.08	2700
^{94}Mo	2.027	10.93	-1.542	0.25	–
^{95}Mo	1.047	11.03	-1.537	0.34	1320
^{96}Mo	2.138	11.13	-1.531	0.46	105
^{97}Mo	0.995	11.23	-1.526	0.65	1050
^{98}Mo	2.080	11.33	-1.521	0.87	75

All the available NLD datasets of $^{93-98}\text{Mo}$ are plotted in Fig. 1 along with those obtained from the BSFG model using two parameterizations in Eqs. (1) and (6). The parameters of the BSFG formula (6) together with the D_0 values are taken from Refs. [21,22] and listed in Table 1. Since the new NLD and D_0 data for $^{94-98}\text{Mo}$ are recommended, the old BSFG parametrization in Table 1 is no longer valid. This can be clearly seen in Figs. 1[(b)-(f)] that the BSFG NLDs with parameters in Table 1 (dashed lines) agree with the NLD datasets in 2003 (triangles) and 2006 (circles) only. Hence, the new BSFG parameterization must be performed in order to obtain the best fit to the newly recommended NLD datasets (squares in Fig. 1). In this work, we used the BSFG formula (1) and slightly re-adjusted its parameters to obtain the best fit to the new NLD datasets. These new BSFG parameters and D_0^{rec} values are listed in Table 2 in comparison with those taken from RIPL-3

Table 2 Parameters of the BSFG formula (1) used in this work in comparison with those taken from RIPL-3 database [38]

RIPL-3					
Nucleus	δW (MeV)	γ (MeV ⁻¹)	\tilde{a} (MeV ⁻¹)	E_1 (MeV)	D_0 (eV)
⁹³ Mo	-1.843	0.091	10.370	-0.095	2700
⁹⁴ Mo	-0.473	—	—	—	—
⁹⁵ Mo	0.097	0.090	10.892	0.022	1320
⁹⁶ Mo	1.025	0.090	10.709	1.141	105
⁹⁷ Mo	1.700	0.089	10.745	-0.131	1050
⁹⁸ Mo	2.453	0.089	10.811	1.024	75
This work					
Nucleus	δW (MeV)	γ (MeV ⁻¹)	\tilde{a} (MeV ⁻¹)	E_1 (MeV)	D_0 (eV)
⁹³ Mo	-1.843	0.101	10.070	0.055	2700
⁹⁴ Mo	-0.473	0.081	10.495	0.801	81
⁹⁵ Mo	0.097	0.110	11.152	0.217	831
⁹⁶ Mo	1.025	0.080	10.509	0.879	66
⁹⁷ Mo	1.700	0.089	10.545	-0.226	661
⁹⁸ Mo	2.453	0.036	11.071	0.764	47

database [38]. It is clearly seen in Figs. 1(b)-(f) that the BSFG NLDs obtained using these new parameters (solid lines) fit very well the new datasets (squares), except for ⁹³Mo. For ⁹³Mo, there exists only one dataset in 2006. Moreover, the BSFG with parametrization in Table 1 even underestimates the experimental data below about 4 MeV. Therefore, we have to readjust the BSFG parameters to obtain the best fit to the experimental data in the entire data range (from about 1 – 8 MeV) (see Fig. 1(a) and Table 1). In Fig. 2, we plot the extension of the BSFG NLDs with new parameters up to about 120 MeV. Obviously, the new BSFG NLDs reproduce very well the slope of the experimental data.

The empirical heat capacities of ^{93–98}Mo calculated using the partition function (8) and the exp+BSFG NLDs in Fig. 2 are plotted in Fig. 3 versus those taken from previous studies in Refs. [21, 22]. In this figure, the heat capacities taken from Fig. 3 of Ref. [22] (dashed lines) show a very strong S-shape, whereas those taken from Fig. 10 of Ref. [21] exhibit mostly none S-shape. This distinct difference between these two heat capacities is quite strange because they are calculated using the same exp+BSFG NLD data (circles in Fig. 1) plus the same BSFG NLDs (dashed lines in Fig. 1). The results obtained are almost coincided with those taken from Fig. 10 of [21]. We have also performed another test that we take the solid lines (exp+FG) in Fig. 2 of Ref. [22] and re-calculate the heat capacities. However, we cannot reproduce the exp+FG heat capacities

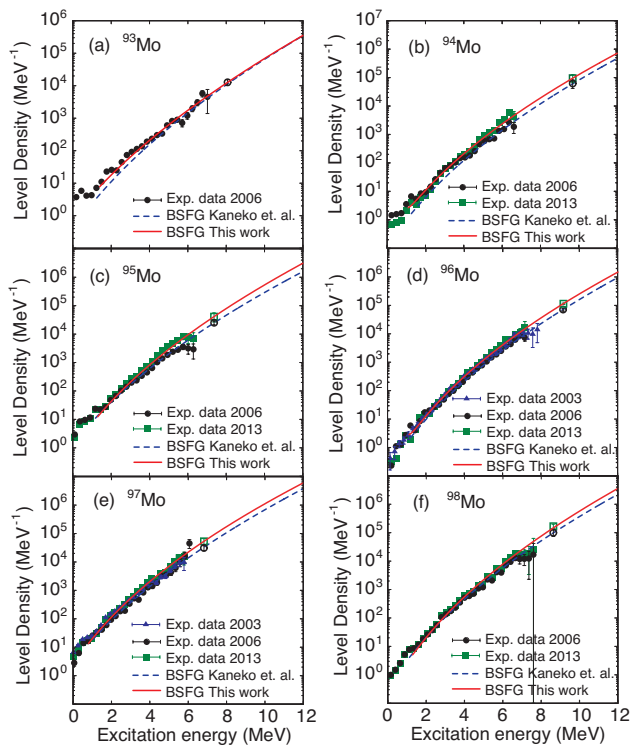


Fig. 1 Experimental and BSFG NLDs as functions of excitation energy for ^{93–98}Mo. The filled triangles and circles (with error bars) are the NLD data taken from Refs. [36] and [21], respectively. The filled squares (with error bars) are the recommended NLD data taken from Refs. [25, 37]. The open circles are the NLD data at the neutron binding energy B_n taken from Fig. 4 of Ref. [21]. The open squares are the NLD data at the neutron binding energy B_n calculated from the recommended D_0 data in Table I of Ref. [25] using the BSFG parameters taken from Table 2. The dashed and solid lines are the NLDs obtained by using the BSFG formulae (6) and (1) with parameters listed in Tables 1 and 2, respectively.

in Ref. [22]. This examination suggests that there might be an error in the numerical calculation of heat capacities in Ref. [22]. By using the new NLD and BSFG data in Fig. 2, the obtained heat capacities (solid lines in Fig. 3) show a qualitative difference with those taken from two previous studies, namely the S-shape is observed in even-even ^{94,96,98}Mo nuclei (see the heat capacities around the region indicated by the arrows in Fig. 3), whereas it is invisible in odd-A ^{93,95,97}Mo isotopes. In addition, the new S-shape observed in even-even nuclei is stronger than that seen in Ref. [21] but weaker than that predicted in Ref. [22]. This result is reasonable because of two reasons. The first reason is that the even-even nuclei often exhibit stronger pairing correlations than the odd ones. The second reason is that the even ^{94,96,98}Mo nuclei are deformed in its ground state because their experimental quadrupole deformation parameters β_2 are 0.1511 ± 0.0016 , 0.1715 ± 0.0014 , and 0.1691 ± 0.0017 , respectively [39]. It is known that de-

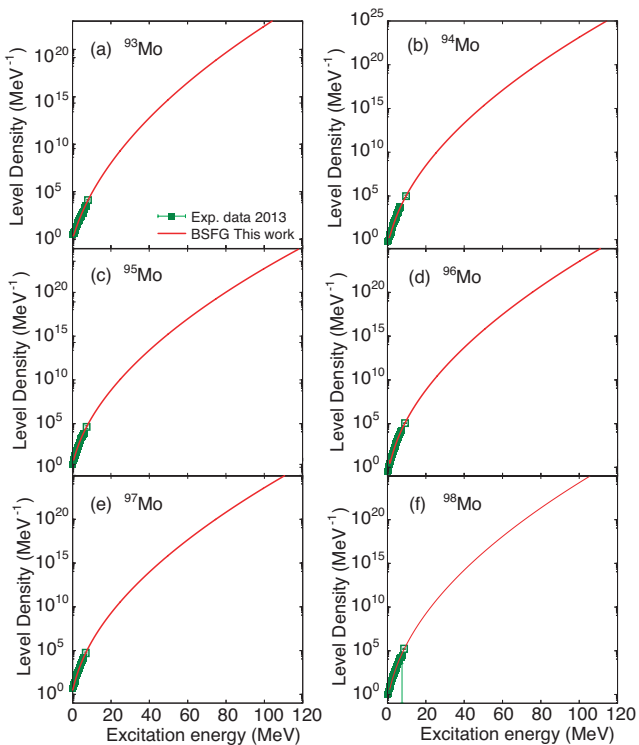


Fig. 2 Experimental and BSFG NLDs as functions of excitation energy up to 120 MeV for $^{93-98}\text{Mo}$. Experimental data (squares) are taken from the recommended values in Refs. [25,37], whereas the BSFG NLDs (solid lines) are calculated using Eq. 1 with parameters listed in Table 1.

formed nuclei always exhibit weaker pairing correlations than spherical ones [24]. This result also suggests that the strong S-shaped heat capacities obtained for odd $^{93,95,97}\text{Mo}$ nuclei in Ref. [22] should be re-investigated. In other words, the newly recommended NLD data in Ref. [25] reflect the correct behavior of nuclear heat capacities in even and odd Molybdenum isotopes and should be used later on for the comparison with the theoretical calculations.

4 Conclusions

The present work re-investigates the empirical heat capacities of $^{93-98}\text{Mo}$ nuclei extracted from the experimental NLDs below the neutron binding energy B_n combined with the BSFG model for the energy above B_n and up to about 120 MeV. For this purpose, the newly updated and recommended NLD data in 2013 have been used and combined with the BSFG NLD with energy-dependent level density parameter and new parameterization. The results obtained indicate that the heat capacities of even $^{94,96,98}\text{Mo}$ nuclei show a more pronounced S-shape than those in odd $^{93,95,97}\text{Mo}$ isotopes. This finding is qualitatively different with those

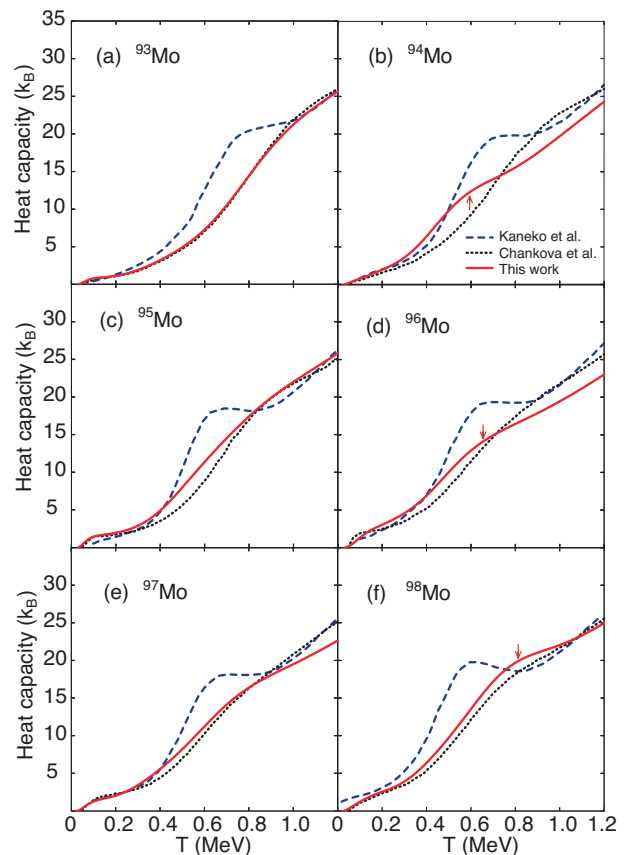


Fig. 3 Empirical heat capacities as functions of temperature T for $^{93-98}\text{Mo}$. The dashed lines present the exp+FG heat capacities taken from Fig. 3 of Ref. [22], whereas the dotted lines denote those taken from Fig. 10 of Ref. [21]. The solid lines stand for the results obtained within the present work by using the new exp+BSFG NLDs in Fig. 2. The red arrows denote the region where the S-shaped heat capacity is observed within the present work.

obtained in two previous studies in Refs. [21,22], in which the old NLD data and the BSFG NLD with energy-independent level density parameter are used. In particular, the present work suggests that the strong S-shape observed in the heat capacities of both even and odd Molybdenum isotopes in Ref. [22] might be caused by an error in the numerical calculations, which should be re-investigated. Finally, to obtain the correct behavior of nuclear heat capacity and associated pairing phase transition, one should use the correct NLD data and the best fitted BSFG NLD in the entire region where the experimental data are available.

Acknowledgements The authors wish to thank University of Khanh Hoa for supporting through the research project No. KHTN-20.01. This work is funded by the National Foundation for Science and Technology Development (NAFOSTED) of Vietnam under Grant No. 103.04-2019.371.

References

1. H. A. Bethe, An attempt to calculate the number of energy levels of a heavy nucleus, *Phys. Rev.* **50**, 332 (1936).
2. T. Rauscher, F. K. Thielemann, and K. L. Kratz, Nuclear level density and the determination of thermonuclear rates for astrophysics, *Phys. Rev. C* **56**, 1613 (1997).
3. T. Rauscher, F. K. Thielemann, Astrophysical reaction rates from statistical model calculations, *At. Data Nucl. Data Tables* **75**, 1 (2000).
4. N. Quang Hung, N. Dinh Dang, and L.G. Moretto, Pairing in excited nuclei: a review, *Rep. Prog. Phys.* **82**, 056301 (2019).
5. T. Sumaryada and A. Volya, Thermodynamics of pairing in mesoscopic systems, *Phys. Rev. C* **76**, 024319 (2007).
6. N. Quang Hung and N. Dinh Dang, Exact and approximate ensemble treatments of thermal pairing in a multi-level model, *Phys. Rev. C* **79**, 054328 (2009).
7. N. Quang Hung, N. Dinh Dang, and L.T. Quynh Huong, Simultaneous microscopic description of nuclear level density and radiative strength function, *Phys. Rev. Lett.* **118**, 022502 (2017).
8. L. Henden et al., On the relation between the statistical γ -decay and the level density in ^{162}Dy , *Nucl. Phys. A* **589**, 249 (1995).
9. T. S. Tveter et al., Observation of fine structure in nuclear level densities and γ -ray strength functions, *Phys. Rev. Lett.* **77**, 2404 (1996).
10. A. Voinov et al., γ -ray strength function and pygmy resonance in rare earth nuclei, *Phys. Rev. C* **63**, 044313 (2001).
11. U. Agvaanluvsan et al., Level densities and γ -ray strength functions in $^{170,171,172}\text{Yb}$, *Phys. Rev. C* **70**, 054611 (2004).
12. M. Guttormsen et al., Experimental level densities of atomic nuclei, *Eur. Phys. J. A* **51**, 170 (2015).
13. E. Melby et al., Thermal and electromagnetic properties of ^{166}Er and ^{167}Er , *Phys. Rev. C* **63**, 044309 (2001).
14. M. Guttormsen et al., Constant-temperature level densities in the quasicontinuum of Th and U isotopes, *Phys. Rev. C* **88**, 024307 (2013).
15. A. Gilbert and A.G.W. Cameron, A composite nuclear-level density formula with shell corrections, *Can. J. Phys.* **43**, 1446 (1965).
16. E. Melby et al., Observation of thermodynamical properties in the ^{162}Dy , ^{166}Er , and ^{172}Yb nuclei, *Phys. Rev. Lett.* **83**, 3150 (1999).
17. M. Guttormsen et al., Entropy in hot $^{161,162}\text{Dy}$ and $^{171,172}\text{Yb}$ nuclei, *Phys. Rev. C* **62**, 024306 (2000).
18. J. L. Egido, L. M. Robledo, and V. Martin, Behavior of shell effects with the excitation energy in atomic nuclei, *Phys. Rev. Lett.* **85**, 26 (2000).
19. S. Liu and Y. Alhassid, Signature of a pairing transition in the heat capacity of finite nuclei, *Phys. Rev. Lett.* **87**, 022501 (2001).
20. A. Schiller et al., Critical temperature for quenching of pair correlations, *Phys. Rev. C* **63**, 021306 (2001).
21. R. Chankova et al., Level densities and thermodynamical quantities of heated $^{93-98}\text{Mo}$ isotopes, *Phys. Rev. C* **73**, 034311 (2006).
22. K. Kaneko et al., Breaking of nucleon Cooper pairs at finite temperature in $^{93-98}\text{Mo}$, *Phys. Rev. C* **74**, 024325 (2006).
23. B. Dey et al., Level density and thermodynamics in the hot rotating ^{96}Tc nucleus, *Phys. Rev. C* **96**, 054326 (2017).
24. B. Dey et al., S-shaped heat capacity in an odd-odd deformed nucleus, *Phys. Lett. B* **789**, 634 (2019).
25. H. Utsunomiya et al., Photoneutron cross sections for Mo isotopes: A step toward a unified understanding of (γ, n) and (n, γ) reactions, *Phys. Rev. C* **88**, 015805 (2013).
26. <https://www-nds.iaea.org/RIPL-1>.
27. <https://www-nds.iaea.org/RIPL-2>.
28. A. V. Ignatyuk, G. N. Smirenkin, and A. S. Tishin, Phenomenological description of the energy dependence of the level density parameter, *Yad. Fiz.* **21**, 485 (1975) [*Sov. J. Nucl. Phys.* **21** 255].
29. A. V. Ignatyuk, K. K. Istekov, and G. N. Smirenkin, Role of the collective effects in a systematics of nuclear level density, *Yad. Fiz.* **29**, 875 (1979) [*Sov. J. Nucl. Phys.* **29** 450].
30. T. V. Egidy and D. Bucurescu, Systematics of nuclear level density parameters, *Phys. Rev. C* **72**, 044311 (2005); *ibid. Phys. Rev. C* **73**, 049901 (2006).
31. A. C. Larsen et al., Transitional γ strength in Cd isotopes, *Phys. Rev. C* **87**, 014319 (2013).
32. T. G. Tornyi et al., Level density and γ -ray strength function in the odd-odd ^{238}Np nucleus, *Phys. Rev. C* **89**, 044323 (2014).
33. A. Bohr and B. R. Mottelson, *Nuclear Structure: Volume 1*, 471, Benjamin, New York (1969).
34. N. Quang Hung and N. Dinh Dang, Canonical and microcanonical ensemble descriptions of thermal pairing within BCS and quasiparticle random-phase approximation, *Phys. Rev. C* **81**, 057302 (2010).
35. N. Quang Hung and N. Dinh Dang, Thermodynamic properties of hot nuclei within the self-consistent quasiparticle random-phase approximation, *Phys. Rev. C* **82**, 044316 (2010).
36. A. Schiller et al., Level densities in $^{56,57}\text{Fe}$ and $^{96,97}\text{Mo}$, *Phys. Rev. C* **68**, 054326 (2003).
37. <https://www.mn.uio.no/fysikk/english/research/about/infrastructure/ocl/nuclear-physics-research/compilation/>.
38. <https://www-nds.iaea.org/RIPL-3/>.
39. <https://www.nndc.bnl.gov/nudat2/>.